

Effect of dopant valence state of Mn-ions on the microstructures and nonlinear properties of microwave sintered ZnO-V₂O₅ Varistors

CHANG-SHUN CHEN

Department of Mechanical Engineering, Hwa-Hsia College of Technology and Commerce, Taipei 235, Taiwan, ROC

E-mail: cschen@cc.hwh.edu.tw

In this study, the effect of dopant valence state of Mn-species on the microstructure and conduction behavior of microwave sintered ZnO-V₂O₅ ceramics was analyzed. Microwave sintering can markedly enhance the densification rate of ZnO-V₂O₅ ceramics, regardless the valence state of Mn-species incorporated. But only the samples doped with low valences Mn-ions (Mn²⁺ or Mn^{2.66+}) exhibit large nonlinear coefficient ($\alpha = 21.9$) with low leakage current density, whereas the ZnO-V₂O₅ ceramics added with high valence Mn-ions (Mn⁴⁺) show inferior nonohmic behaviors with high leakage current density under the same sintering conditions. Restated, the valence state of Mn-species incorporated in ZnO-V₂O₅ ceramics, insignificantly alters the grain growth behavior but markedly modifies their nonlinear electrical properties. © 2003 Kluwer Academic Publishers

1. Introduction

Zinc Oxide ceramics are well known as varistor materials because of their excellent nonohmic properties in current-voltage (*I-V*) characteristics. These nonlinear electrical characteristics are fundamentally attributed to the Schottky barrier nature of the grain boundary layer between the relatively conducting ZnO grains [1, 2]. The large ionic radius additives such as Bi, Pr, Sr and Ba segregate at the grain boundaries and form an electronic conduction barrier between n-type semi conductive ZnO grains [3, 4], acting as effective “varistor-forming” ingredients.

The transition metal ion additives such as Mn and Co [5–15], that generate trapped states both in the grain interiors as well as in grain boundary regions, act as nonohmic property enhancers. Pike *et al.* [11] proposed that Mn enhanced the production of holes during electrical breakdown, improved the nonlinearity of ZnO varistors. Shen [13] proposed that, the composition of ZnO varistors with added Co and Mn ions of high-valence-state (Co³⁺ and Mn⁴⁺), would deduced to result in higher donor density, trap density, barrier height and leakage current, but a lower nonlinearity coefficient in comparison with that of ZnO varistors with added Co and Mn ions of low-valence-state (Co²⁺ and Mn²⁺). H.-H. Hng *et al.* [14, 15] suggested that there were a new oxide compound composed of zinc, vanadium and manganese in ZnO-V₂O₅-MnO₂ system, which possessed obviously nonlinear characteristics. However, the explanation on how the incorporation of transition metal ions influences the nonohmic electrical properties of ZnO materials is still not clear yet.

In the previous study [16–19], we observed that the V₂O₅ additives can markedly enhance the microwave sintering of ZnO materials and the Mn₃O₄-dopants can substantially improve the nonlinear electrical behavior of these materials. In this study, we further investigated the influence of the valence state of the Mn-ions on the microstructure characteristics and the nonlinear current-voltage (*I-V*) of ZnO-V₂O₅ materials.

2. Experimental procedures

Extra pure ZnO varistor powders (>99.9%), containing 0.5 mol% V₂O₅ and 0.9 mol.% Mn-ions, were used to prepare varistor materials by mixed oxide process. The Mn-ions were added in form as Mn(CH₃COO)₂·4H₂O (Mn²⁺), Mn₃O₄ (Mn^{2.66+}) or MnO₂ (Mn⁴⁺). The mixtures were ball-milled in a plastic jar, using zirconia balls and deionized water, for 8 h. After the mixtures were filtered and dried, they were calcined at 700°C in air for 2 h, followed by pulverization in a ball-mill for 8 h to around 1.0 μm size and then uniaxially pressed at 750 kgf/cm² into a disk of 8 mm in diameter and 2 mm in thickness. The green pellets, around 60% of theoretical density (5.675 g/cm³) was microwave sintered (ms) at 900°C for 30 min in an applicator made of WR284 waveguide, using a 2.45 GHz microwave generated from a commercial source (Gerling GL107 magnetron). The temperature profile was measured using Pt-13% Rh thermocouple, placed near the sample surface. The heating rate was controlled at 60°C/min and the cooling rate was controlled at 80°C/min for sintering temperature above 500°C. For comparison, the samples were also prepared by conventional furnace

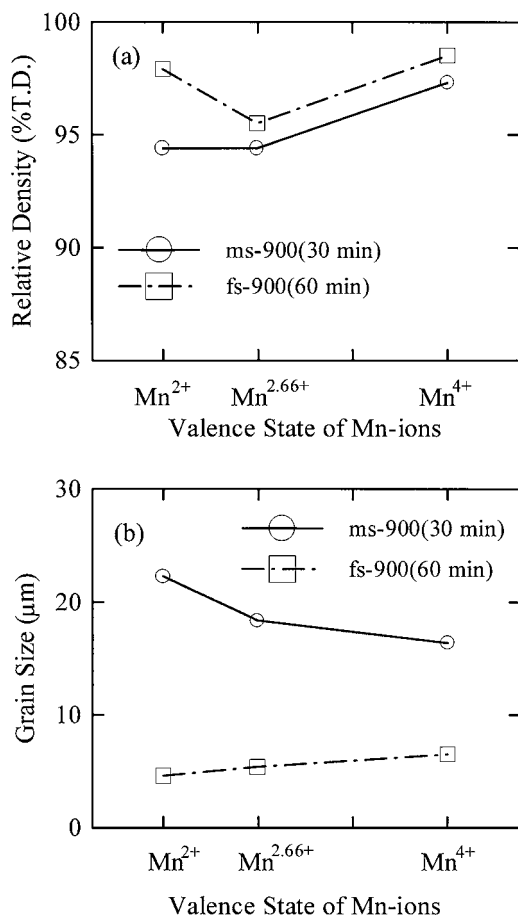


Figure 1 The (a) sintered density and (b) grain size of Mn-doped ZnO materials prepared by microwave sintering (ms, 900°C for 30 min) and furnace sintering (fs, 900°C for 60 min) process. (Mn-species are incorporated either as Mn(CH₃COO)₂·4H₂O: Mn²⁺, Mn₃O₄: Mn^{2.66+} or MnO₂: Mn⁴⁺).

sintering process (fs), that is, densification at 900°C for 60 min. or 4 hours in an electrical furnace. The heating rate and the cooling rate were 5°C/min.

The crystal structure of the sintering samples was examined using Shimadzu (XD-5) X-ray diffractometer (XRD) and the microstructure were examined using Joel JSM-840A scanning electron microscope (SEM). The voltage-current (*V-I*) properties of these samples

were recorded using Keithley 237 *I-V* electrometer in dc source after the In-Ga (40:60) alloy was rubbed onto the sample surface to serve as electrodes. The breakdown electric field (*V_{bk}*) was measured at current density of 1.0 mA/cm², nonlinear coefficient (α) was estimated for a current density ranges from 1.0 mA/cm² to 10 mA/cm² and leakage current density (*J_L*) was defined as the current density at applied field of 10 V/mm. The capacitance-voltage (*C-V*) measurements were made at room temperature using HP4274A capacitance meter. The electrical characteristics, including Schottky barrier height (Φ_b) donor density (*N_d*) and surface state density (*N_s*), were determined from capacitance-voltage (*C-V*) data, using the model proposed by Mukae *et al.* [20].

3. Results and discussion

3.1. Sintering behavior

According to previous studies [14–17], the V₂O₅ additives can markedly enhance the densification rate of the ZnO materials. Such a phenomenon does not change with the valence state of the Mn-species incorporated. Fig. 1a shows that both microwave sintered (ms) and furnace sintered (fs) samples containing the Mn²⁺-, Mn^{2.66+}- or Mn⁴⁺-species can reach a high density as 95% theoretical density (T.D.) when they are densified at 900°C. However, furnace-sintering process still needs longer soaking period than the microwave sintering process to attain the same sintered density. The morphology and grain growth behaviors of these ZnO materials containing high-valence-Mn (Mn⁴⁺) additives are significantly different from the characteristics of the samples containing low-valence-Mn (Mn²⁺ and Mn^{2.66+}) additives. SEM examinations show that, when furnace sintered at 900°C for 60 minutes, the samples doped with Mn⁴⁺-ions still contain numerous sub-micron sized second phase particles with grain size around 6.4 μm (Fig. 2a), whereas the samples doped with Mn²⁺- and Mn^{2.66+}-ions have already developed a single-phase uniform microstructure with grain size around 4–5 μm (Fig. 2c). Abnormal grain growth phenomenon occurs frequently for these

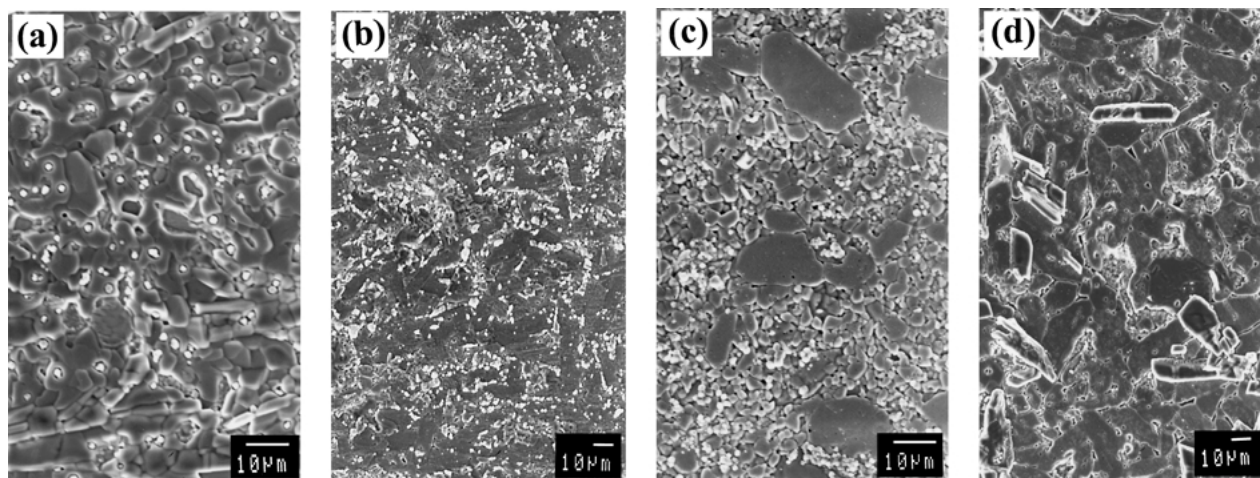


Figure 2 The SEM micrographs of Mn⁴⁺-ions doped ZnO materials (a) furnace sintered (fs) at 900°C for 60 min, (b) microwave sintered (ms) at 900°C for 30 min and Mn^{2.66+}-ions doped ZnO materials (c) furnace sintered (fs) at 900°C for 60 min, (d) microwave sintered (ms) at 900°C for 30 min.

samples. These results reveal that the reactive mechanisms of high-valence-Mn doped (Mn^{4+})-ZnO materials were different from those of low-valence-Mn doped (Mn^{2+} and $Mn^{2.66+}$)-ZnO materials. Such phenomenon will be discussed later.

Similar behavior is observed for the ZnO materials microwave sintered at $900^{\circ}C$ for 30 minutes, as shown in Fig. 2b and d. The morphology of high-valence-Mn (Mn^{4+}) (Fig. 2b) incorporated samples is markedly different from that of the low-valence-Mn (Mn^{2+} and $Mn^{2.66+}$) incorporated samples (Fig. 2d). The former contains large number of sub-micron sized particles, whereas the latter contains only ZnO grains. Moreover, the grain size of the microwave sintered ZnO materials, which is around $18\text{--}23\ \mu m$, is markedly larger and the granular distribution of these materials is much more uniformed, as compared with that of the furnace sintered samples (cf. Fig. 1b). These results reveal that microwave-sintering process has enhanced the grain growth rate of the ZnO materials such that all of microwave sintered samples possess a well-developed microstructure.

Typical phase constituent of these materials is represented by the X-ray diffraction patterns of the $900^{\circ}C$ (30 min.) microwave sintered ZnO-0.5 mol% V_2O_5 -0.9 mol% MnO_x materials. Fig. 3 reveals that besides the main hexagonal ZnO phase and minor $Zn_3(VO_4)_2$ (JCPDS 19-1470) secondary phase, no other phases are observable. The EDAX for low-valence-Mn (Mn^{2+} and $Mn^{2.66+}$) doped samples, which were microwave sintered at $900^{\circ}C$ for 30 minutes and under thermally etched at $850^{\circ}C$ for 30 minutes after polishing, is shown in Fig. 4. EDAX spectra for inter-granular and trans-granular fractured surfaces, shown as spectra 1 and 2 (Fig. 4a), respectively, indicate that the grain boundaries contain large proportion of V- and Mn-species, which are uniformly distributed, whereas the grain interiors contain only minute amount of Mn-species, in addition to the main constituents (ZnO). This phenomenon is in accord with the fact that the V_2O_5 -species are added as the main liquid phase additives and the MnO_x -species are included as the main surface

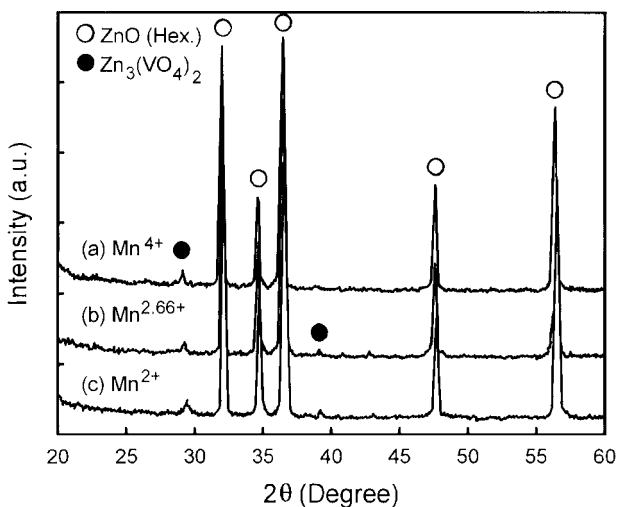


Figure 3 The X-ray diffraction patterns ($Cu\ K\alpha$) of ZnO materials microwave sintered at $900^{\circ}C$ for 30 min, (a) Mn^{2+} , (b) $Mn^{2.66+}$ and (c) Mn^{4+} , respectively.

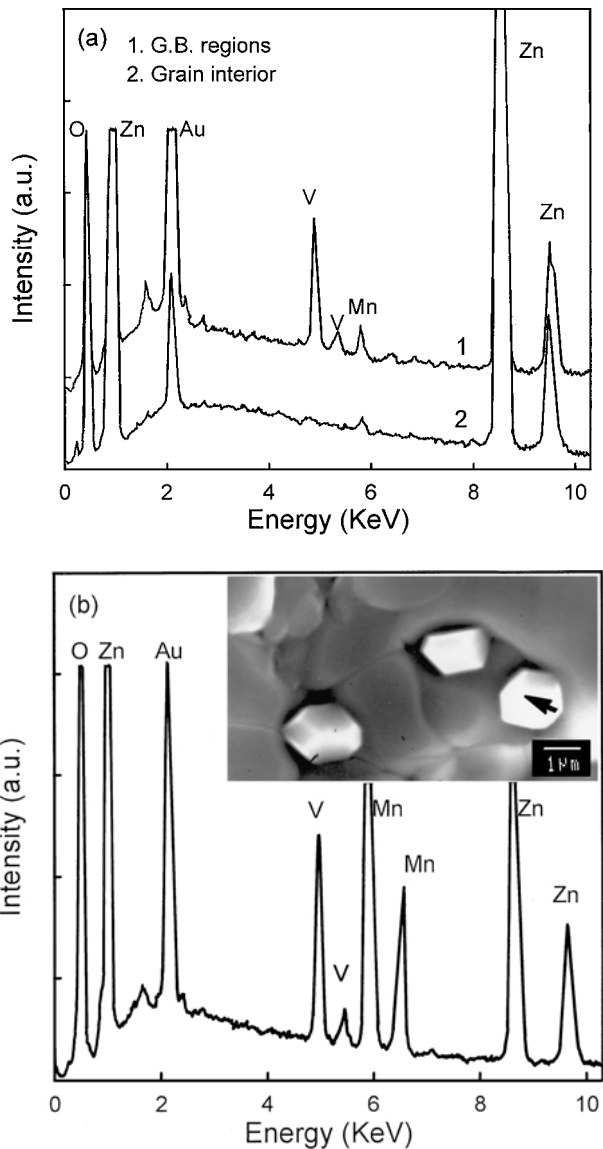


Figure 4 The EDAX patterns of (a) Mn^{2+} (or $Mn^{2.66+}$) doped ZnO- V_2O_5 materials microwave sintered at $900^{\circ}C$ for 30 min, the grain interior and grain boundary, and those of (b) Mn^{4+} -doped ZnO- V_2O_5 materials microwave sintered at $900^{\circ}C$ for 30 min.

state modifiers. By contrast, the grain junctions of the high-valence-Mn (Mn^{4+}) doped samples contain large amount of sub-micron sized particles no matter whether the samples are microwave sintered (Fig. 4b) or furnace sintered (not shown). The EDAX spectra focus to these sub-micron particles at the grain junctions indicate that these particles were primarily Mn-rich species in addition to the V- and Zn-species. These results imply that high-valence-Mn (Mn^{4+}) dopants mainly reacted with ZnO- V_2O_5 at grain junction regions during liquid phase sintering periods. These second phase particles either was an oxide that composed of zinc, vanadium and manganese or was a zinc vanadate phase with a solid solution of manganese [15]. Such results reveal that high-valence Mn-ions (Mn^{4+}) are not easy to diffuse into ZnO grain interiors as the bulk dopants generating trapped states.

3.2. Electrical properties

The valence state of Mn-species imposes significant effect on the electrical properties of the ZnO-materials.

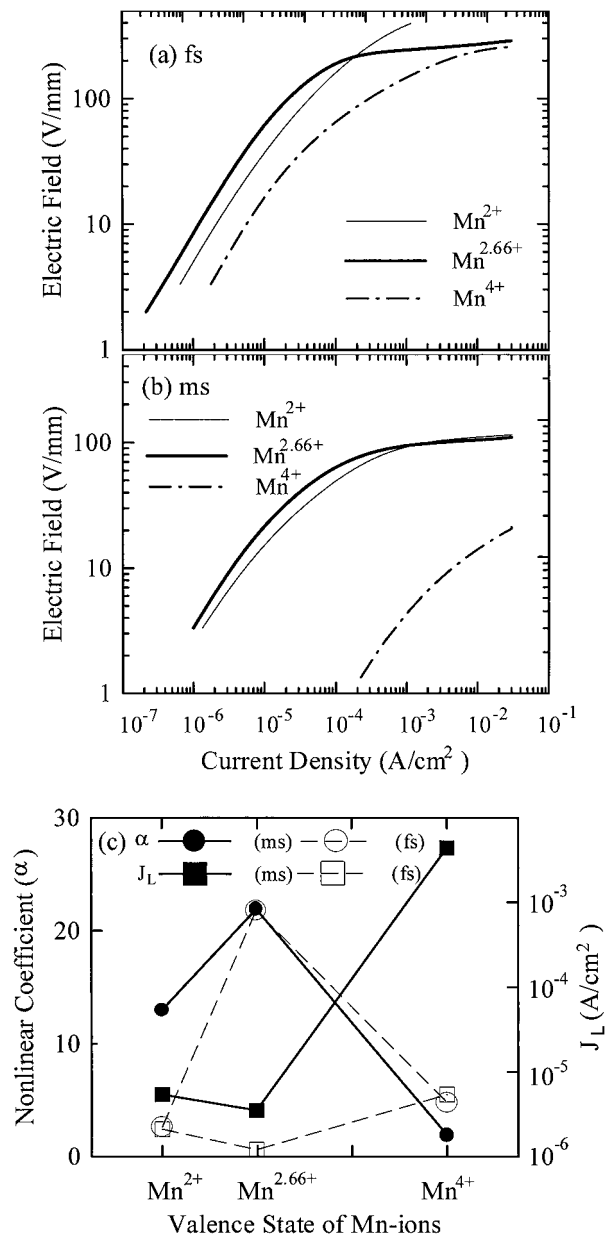


Figure 5 The current density-electric field (J - E) curves of the Mn-ions doped ZnO materials (a) furnace sintered (fs) at 900°C for 60 min, (b) microwave sintered (ms) at 900°C for 30 min and (c) corresponding nonlinear coefficient (α) and leakage current density (J_L).

As shown in Fig. 5a for the electrical behaviors of the Mn-doped ZnO materials furnace sintered (fs) at 900°C (60 min), the samples containing high-valence-Mn exhibit a large leakage current density ($J_L = 5.4 \times 10^{-6}$ A/cm²) and deteriorated nonohmic behaviors ($\alpha = 4.8$). Only the low-valence-Mn additives can suppress the leakage current density (J_L) and enhance the nonlinear of the ZnO-V₂O₅ materials. Moreover, the nonohmic characteristics of the Mn^{2.66+}-doped materials are markedly better than that of the Mn²⁺-doped samples, (viz. $\alpha = 21.8$ for Mn^{2.66+}-added materials and $\alpha = 2.6$ for Mn²⁺-added samples).

Similar behavior is observed for the materials microwave sintered at 900°C for 30 minutes. Fig. 5b reveals that the low-valence-Mn additives (Mn²⁺ and Mn^{2.66+}) have markedly suppressed the leakage current density (J_L) of the ZnO-0.5 mol% V₂O₅ materials, resulting in prominent nonohmic characteris-

tics (solid curves). By contrast, the high-valence-Mn additives (Mn⁴⁺) are completely unsuccessful to improve the electrical properties of the ZnO-0.5 mol% V₂O₅ materials, which possess large leakage current density and deteriorated nonohmic behaviors. The nonlinearity (α) and leakage current density (J_L) estimated from these J - E curves are $\alpha = 20$ -21.9 and $J_L = 3.5 \times 10^{-6} \sim 5.4 \times 10^{-6}$ A/cm² for the low-valence-Mn doped samples and are $\alpha = 1.9$ and $J_L = 4.4 \times 10^{-3}$ A/cm² for the high-valence-Mn doped materials. It is interesting to observe that although Mn²⁺-species incorporated into ZnO-V₂O₅ materials cannot improve their nonohmic characteristics when they are furnace sintered, these species do markedly enhance their nonlinear behavior when the materials are microwave sintered. These results indicate how the fast sintering process induced by the microwave facilitates the formation of non-equilibrium phase structure, resulting in improved nonohmic electrical properties.

The intrinsic electrical parameters derived from capacitance-voltage (C - V) measurements reveal that donor concentration is $N_d = 1.18 \times 10^{18} \sim 1.75 \times 10^{18}$ cm⁻³, surface state density is $N_s = 4.32 \times 10^{11} \sim 5.28 \times 10^{11}$ cm⁻² and potential barrier height is $\Phi_b = 1.18$ -1.70 eV for the microwave sintered (ms) ZnO-V₂O₅ materials doped with low-valence-Mn additives (Mn²⁺ and Mn^{2.66+}) (Table I). By contrast, the high-valence-Mn additives (Mn⁴⁺) possess higher donor concentration ($N_d = 24.9 \times 10^{18}$ cm⁻³) and surface state density ($N_s = 7.94 \times 10^{11}$ cm⁻²) but lower potential barrier height ($\Phi_b = 0.27$ eV), which are completely unsuccessful to improve the electrical properties of the ZnO-0.5 mol% V₂O₅ materials. Restated, the low-valence-Mn doped samples exhibit nonohmic characteristics significantly superior to the high-valence-Mn (Mn⁴⁺) doped ones.

In order to know how the high-valence-Mn additives (Mn⁴⁺) are unsuccessful to improve the electrical properties of the ZnO-0.5 mol% V₂O₅ materials under densification at 900°C for 60 min. in an electrical furnace or at 900°C for 30 min. in microwave sintering chamber, the sintering periods of the samples doped with high-valence-Mn (Mn⁴⁺) are lengthened, that is, densification at 900°C for 4 hours in an electrical furnace. SEM examinations show that, in addition to grain growth (grain size around 24.0 μ m), these samples contain minute amount of sub-micron sized second phase

TABLE I Effect of dopant valence-state of Mn-ions on the microwave sintered ZnO-0.5 mol% V₂O₅ ceramics (0.9 mol% of Mn-ions)

Dopant ^a	Mn ²⁺	Mn ^{2.66+}	Mn ⁴⁺
V_{bk} (V/mm)	92.2	94	4.3
J_L (μ A/cm ²)	5.4	3.5	4.4×10^3
α	20	21.9	1.9
N_d (10 ¹⁸ /cm ³)	1.75	1.18	24.9
N_s (10 ¹¹ /cm ²)	5.28	4.32	7.94
Φ_b (eV)	1.70	1.18	0.27
G.S. (μ m)	22.3	18.4	16.4
Density (%T.D.)	94.4	94.4	97.3

^aMn²⁺ is added in a form of Mn(CH₃COO)₂·4H₂O; Mn^{2.66+} are added in a form of Mn₃O₄ and Mn⁴⁺ are added in a form of MnO₂.

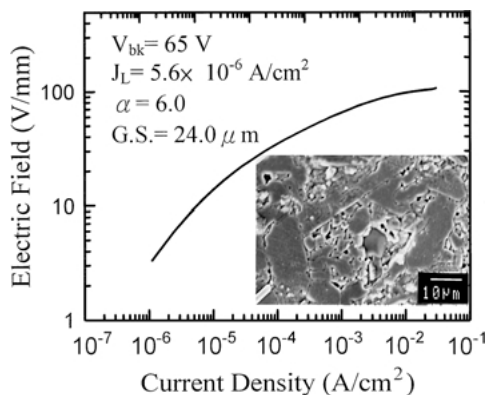


Figure 6 The current density-electric field (J - E) curves of the high-valence-Mn (Mn^{4+}) doped $\text{ZnO-V}_2\text{O}_5$ materials furnace sintered (fs) at 900°C for 4 hours.

particles (Fig. 6) compare to those shorter sintering periods samples (Fig. 2a and b). Abnormal grain growth phenomenon is also observed in these samples.

The electrical properties (J - E) of these samples are shown in Fig. 6. The breakdown voltage (V_{bk}), nonlinearity (α) and leakage current density (J_{L}) are $V_{\text{bk}} = 65$ V/mm, $\alpha = 6.0$ and $J_{\text{L}} = 5.6 \times 10^{-6}$ A/cm², respectively. The intrinsic electrical parameters which include donor concentration ($N_{\text{d}} = 2.17 \times 10^{18}$ cm⁻³), surface state density ($N_{\text{s}} = 5.91 \times 10^{11}$ cm⁻²) and potential barrier height ($\Phi_{\text{b}} = 1.72$ eV). These results reveal that the samples possess higher breakdown voltage (V_{bk}), nonlinearity (α) and lower leakage current density (J_{L}) under longer sintering periods (4 hours). The intrinsic electrical parameters are lower donor concentration and surface state density, but higher potential barrier height compare to those shorter sintering periods samples (60 min. or 30 min.).

3.3. Diffusion couples

The above described results indicate that the valence state of Mn-species significantly affect the characteristics of the $\text{ZnO-V}_2\text{O}_5$ materials. To understand the reactions involved, a diffusion-couple experiment is performed. In this experiment, green pellets of $\text{ZnO-1.0 mol\% V}_2\text{O}_5$ materials (10 mm dia. \times 2 mm height)

were first made, followed by compacting the MnO_x pellets (~ 2 mm height) on top of the green $\text{ZnO-V}_2\text{O}_5$ samples. The green compacts consisting of MnO_x and $\text{ZnO-V}_2\text{O}_5$ double layer were then fired in an electrical furnace with a condition similar to that for sintering the $\text{ZnO-V}_2\text{O}_5$ samples, that is, 1000°C (60 min). The MnO_x and $\text{ZnO-V}_2\text{O}_5$ blocks were then split. The morphology and composition of the surface near the MnO_x - and -ZnO interface of the diffusion couple were then examined.

The interfacial morphology on the $\text{ZnO-V}_2\text{O}_5$ block of the diffusion couple does not vary with the valence state of MnO_x materials (not shown). Whereas, Fig. 7 indicates that the interfacial morphology on the Mn^{4+} -block of diffusion couple is very much different from those in the Mn^{2+} - and $\text{Mn}^{2.66+}$ -block of diffusion couples. The former still consists of very fine particles whereas the latter contain large grain (~ 10 μm) dense compacts, indicating that the MnO_2 materials are hardly densified. On the other hand, the composition of the interfaces of the diffusion couples examined using EDAX in SEM are varied with the valence state of MnO_x block in the diffusion couples markedly. The Mn-signal is clearly observed only on the surface of the $\text{ZnO-V}_2\text{O}_5$ block in contact with low-valence-Mn block. No Mn-signal is detectable for those in contact with high-valence-Mn block (Fig. 7d). These results infer that the interaction between MnO_x and $\text{ZnO-V}_2\text{O}_5$ materials is pronounced only for Mn^{2+} (or $\text{Mn}^{2.66+}$)- $\text{ZnO(V}_2\text{O}_5)$ diffusion couple and is insignificantly small for Mn^{4+} - $\text{ZnO(V}_2\text{O}_5)$ diffusion couple.

In other words, the Mn^{4+} -ions are not easy to react with the $\text{ZnO-V}_2\text{O}_5$ materials and, therefore, it needs longer sintering periods to behave as surface states. Such phenomenon accounts for the high leakage current density of the Mn^{4+} -ions incorporated $\text{ZnO-V}_2\text{O}_5$ samples under shorter sintering periods is ascribed to high Schottky barrier along grain boundaries is not successfully developed in these samples. As to the factor, which hinders the inter-diffusion between the Mn^{4+} - and Zn^{2+} -species, the difference in ionic size is assumed to be the most probable cause. The size of Mn-ions is $R_{\text{Mn}^{2+}} = 0.80$ \AA , $R_{\text{Mn}^{3+}} = 0.70$ \AA and $R_{\text{Mn}^{4+}} = 0.60$ \AA , whereas the size of Zn-ions is

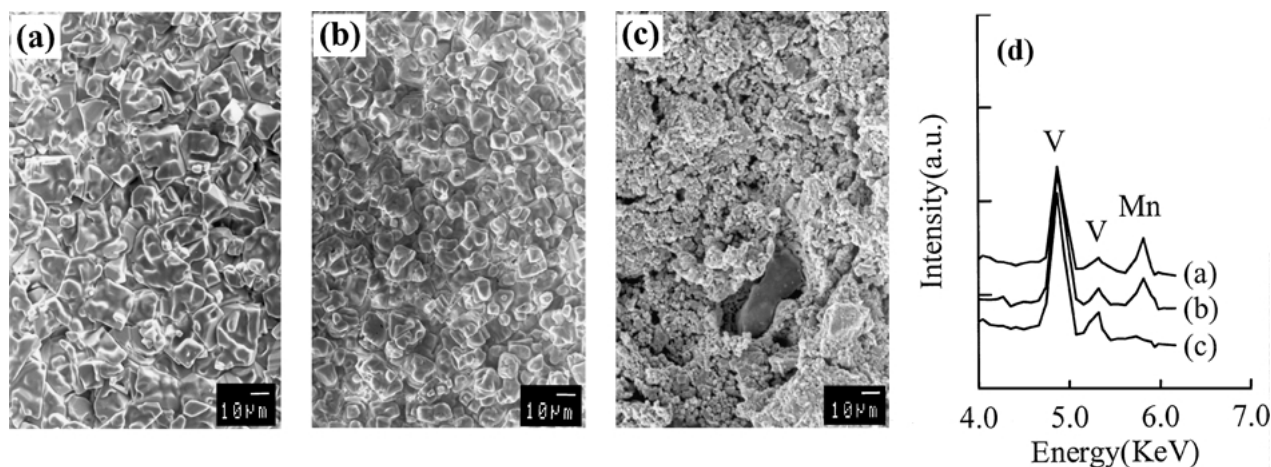


Figure 7 The surface morphology of (a) Mn^{2+} (MnO), (b) $\text{Mn}^{2.66+}$ (Mn_3O_4), (c) Mn^{4+} (MnO_2) and (d) EDAX patterns of MnO_x and $\text{ZnO-V}_2\text{O}_5$ diffusion couples at the interface on $\text{ZnO-V}_2\text{O}_5$ -block sintered at 1000°C for 60 min.

$R_{Zn}^{2+} = 0.74 \text{ \AA}$. Large discrepancy between R_{Mn}^{4+} and R_{Zn}^{2+} retards the solubility of Mn^{4+} in $ZnO-V_2O_5$ materials, which markedly suppress the inter-diffusion between the two materials. By contrast, the values of R_{Mn}^{2+} and R_{Mn}^{3+} are very close to that of R_{Zn}^{2+} , implying that inter-diffusion between the two materials can be easily induced and, therefore, the materials' nonlinear electrical properties are markedly improved.

Restates, from the microstructural analysis (XRD, SEM and EDAX), diffusion couples and electrical behaviors of these different valence-state-Mn doped $ZnO-V_2O_5$ materials, it can do some speculations, because of large discrepancy between R_{Mn}^{4+} and R_{Zn}^{2+} , the high-valence-Mn-ions dopant mainly react with zinc- and vanadium-species via eutectically forming as Zn-V-Mn oxides phase instead of forming as solid solution in grain interiors. Accordingly, Mn^{4+} could not modify the electrical behaviors of these $ZnO-V_2O_5$ materials effectively under shorter sintering periods compare to those of low-valence-state Mn-doped (Mn^{2+} and $Mn^{2.66+}$) ZnO materials.

4. Conclusion

Microwave sintering techniques were used to densify the $ZnO-V_2O_5$ ceramics. Effect of valence state of Mn-species on the microstructures and nonlinear electrical behaviors in $ZnO-V_2O_5$ ceramics was analyzed. Microwave sintering has markedly enhanced densification rate. Microstructure (SEM) shows different morphology between high valence (Mn^{4+}) and low valence (Mn^{2+} and $Mn^{2.66+}$) Mn-ions added of these $ZnO-V_2O_5$ ceramics. The low-valence-Mn ion additives result in highly nonohmic $I-V$ behaviors. The large nonlinear coefficient as $\alpha = 21.9$ is achieved for 0.9 at.% $Mn^{2.66+}$ -ions (Mn_3O_4) doped $ZnO-V_2O_5$, which are materials microwave sintered at 900° for 30 min. These sample posses lower leakage current density, smaller donor density and less surface state density, but have higher barrier height. Contrast, the $ZnO-V_2O_5$ ceramics doped with high valence Mn-ions (Mn^{4+}) show inferior nonohmic behaviors under the same sintering periods. The samples show higher leakage current density, larger donor density, richer surface state density and corresponding barrier height is lower.

Acknowledgment

Financial support by National Science Council of R.O.C. through the project No. NSC 89-2216-E146-001 is gratefully acknowledged by the authors.

References

1. G. D. MAHAN, L. M. LEVINSON and H. R. PHILIPP, *J. Appl. Phys.* **50** (1979) 2799.
2. G. E. PIKE, *Mater. Res. Soc.* **5** (1982) 367.
3. M. MATSUOKA, *Jpn. J. Appl. Phys.* **10** (1971) 736.
4. K. MUKAE, K. TSUDA and I. NAGASAWA, *ibid.* **16** (1977) 1361.
5. K. KOUMOTOT, N. AOKI, N. KITAORI and H. YANAGIDA, *J. Amer. Ceram. Soc.* **65** (1982) C93.
6. E. D. KIM, C. H. KIM and M. H. OH, *J. Appl. Phys.* **58** (1985) 3231.
7. W. G. CARLSON and T. K. GUPTA, *ibid.* **53** (1982) 5746.
8. F. GREUTER, G. BLATTER, F. STUCKI and M. ROSSINELLI, in "Ceram. Transac.," Vol. 3: Advances in Varistor Technology, edited by L.M. Levinson (American Ceramic Society, Westerville, OH, 1989) p. 31.
9. K. EDA, *J. Appl. Phys.* **49** (1978) 2964.
10. J. M. DRIEAR, J. P. GUERTIN, T. O. SOKOLY and L. B. HACKNEY, in "Advances in Ceramic," Vol. 1, edited by L.M. Levinson (American Ceramic Society, Westerville, OH, 1981) p. 316.
11. G. E. PIKE, S. R. KURTZ, P. L. GOURLEY, H. R. PHILLIP and L. M. LIVINSON, *J. Appl. Phys.* **57** (1985) 5512.
12. G. BLATTER and F. GREUTER, *Phys. Rev. B* **33** (1986) 3952.
13. C.-Y SHEN, L. WU and Y.-C CHEN, *Jpn. J. Appl. Phys.* **32** (1993) 2043.
14. H.-H. HNG and K. M. KNOWLES, *J. Amer. Ceram. Soc.* **83** (2000) 2455.
15. H.-H. HNG, K. M. KNOWLES and P. A. MIDGLEY, *ibid.* **84** (2001) 435.
16. C. S. CHEN, C. T. KUO, T. B. WU and I. N. LIN, *Jpn. J. Appl. Phys.* **36** (1997) 1169.
17. C. T. KUO, C. S. CHEN and I. N. LIN, *J. Amer. Ceram. Soc.* **81** (1998) 2942.
18. *Idem.*, *ibid.* **81** (1998) 2949.
19. J. K. TSAI and T. B. WU, *J. Appl. Phys.* **76** (1994) 4817.
20. K. MUKAE, K. TSUDA and I. NAGASAWA, *ibid.* **50** (1979) 4475.

Received 23 October 2001

and accepted 12 November 2002